Materials Research Proceedings **32** (2023) 167-172 https://doi.org/10.21741/9781644902615-18

Low-temperature superplasticity of Si-added medium-Mn steel

Hyun-Bin Jeong[1,a], Seok-Won Choi[1,b], Seok-Hyeon Kang[1,2,c] and Young-Kook Lee[1,d,*]

[1]Department of Materials Science and Engineering, Yonsei University, Seoul, 03722, Republic of Korea

[2]Current address: Research & Development Division, Hyundai-Steel, Dangjin 31719, Republic of Korea

[a]fenixbin@yonsei.ac.kr, [b]csw526@yonsei.ac.kr, [c]ksh546@hyundai-steel.com, [d]yklee@yonsei.ac.kr

Keywords: Low-Temperature Superplasticity, Dynamic Reverse Transformation, Grain Boundary Sliding, High Strength Steel

Abstract. Grain boundary sliding, a deformation mechanism of superplasticity, occurs only at high temperatures, making it difficult for superplastic steels to be practically applied due to high energy consumption and surface oxidation. Therefore, in the present study, we introduce a newly developed Si-added medium-Mn steel, which can be superplastically deformed at such a low temperature of 763 K. The low-temperature superplasticity of this steel was caused by grain boundary sliding between recrystallized α grains and dynamically reverted γ grains. The steel also exhibited high room-temperature tensile strength (1336 MPa) after the superplastic forming simulation.

Introduction

Superplastic materials have drawn significant attention due to high elongation prior to tensile failure, which makes them ideal for making complex-shaped mechanical parts without welding or joining. In particular, superplastic steels have been extensively studied due to low material and production costs, such as high-carbon steel [1-3], duplex stainless steel [4,5], high-specific-strength steel [6], and medium-Mn steel (MMS) [7-12]. However, their practical application is challenging due to their high superplastic deformation temperature (T_s) [7,9]. To overcome the limitation, present authors reported a new Fe-10Mn-3.5Si steel [12], which exhibited superplasticity at 763 K with a strain rate ($\dot{\varepsilon}$) of 1×10^{-3} s^{-1}. The steel has a low material cost and can be produced using a conventional rolling process [12]. Unlike previous superplastic materials with a dual-phase microstructure [7-11], the steel has a single-phase microstructure before plastic deformation [12]. Additionally, after a superplastic forming simulation at 763 K, the steel possesses ultrahigh tensile strength (1336 MPa) at room temperature [12], which far exceeds the tensile strength of Al-added MMS (715 MPa) [9].

Experimental

The ingots of Si-free and Si-added 10Mn steels were produced using an induction melting furnace with an Ar atmosphere. The actual chemical compositions of the steels were Fe-10.5Mn and Fe-10.6Mn-3.5Si (wt%), respectively [12]. After homogenization at 1373 K for 12 h, the ingots were hot-rolled at temperatures ranging from ~1373 K to 1273 K to ~4.0-mm-thick plates, and then air-cooled to room temperature. After surface descaling, the hot-rolled plates were cold-rolled at room temperature to 1.5-mm-thick sheets, which corresponded to thickness reductions of 50%.

For high-temperature tensile testing, tensile specimens with a gauge part of 5.0 × 10.0 × 1.5 mm^3 were machined from the cold-rolled sheets. Uniaxial tensile tests were performed using universal testing machines (MTDI equipped with a high-temperature furnace). Before tensile tests,

tensile specimens were heated to various temperatures at a heating rate of 0.5 K s^{-1}, maintained for 5 min at a given tensile temperature, and then deformed at the initial $\dot{\varepsilon}$ of 1×10^{-3} s^{-1}. A failed specimen was removed from the furnace, followed by air cooling to room temperature.

For the superplastic forming simulation, high-temperature tensile specimens with the gauge part of 20.0 × 10.0 × 1.5 mm^3 were machined. The specimens were strained by ~100% at the T_s of each specimen with an initial $\dot{\varepsilon}$ of 1×10^{-3} s^{-1}. After that, a small-sized tensile specimen was machined from the gauge part of the high-temperature interrupted tensile specimen. The gauge part of the small-sized tensile specimen was 16.0 × 3.0 × 0.8 mm^3. The small-sized tensile specimen was deformed using universal testing machines (Instron 3382) at room temperature with an initial $\dot{\varepsilon}$ of 1×10^{-3} s^{-1}.

The microstructures of the specimens were examined at room temperature using an X-ray diffractometer (XRD; Rigaku, Smartlab) and a field-emission scanning electron microscope (FE-SEM; JEOL, JSM-7001F) equipped with an electron backscattered diffractometer (EBSD; EDAX-TSL, Digiview). For XRD analysis, the specimens were mechanically polished with a suspension of 1 μm diamond particles, and then electropolished in a mixed solution of 90% glacial acetic acid (CH_3COOH) and 10% perchloric acid ($HClO_4$) at 15 V for 1 min to remove the damaged layer. For SEM-EBSD observation, the specimens were polished with a suspension of 0.04 μm colloidal silica particles. The SEM-EBSD operation parameters, such as the accelerating voltage, probe current, working distance, and step size, were set to 20 kV, 12 nA, 15 mm, and 25 nm, respectively.

The phase constituents of the present steels were determined using XRD with Cu-Kα_1 radiation, with a scanning rate, step size, and range of 2° min^{-1}, 0.02°, and 40°-100°, respectively. The volume fraction of γ phase was calculated using the integrated intensity method, which takes into account the integrated intensities of all diffracted peaks. The effect of texture on γ fraction was considered by dividing the integrated intensity of each peak by the pole density of each plane [13].

Results and discussion

All hot-rolled plates had a full α'-martensite microstructure without γ phase due to the high hardenability of the steels used (Fig. 1a [12]). Accordingly, cold-rolled sheets had a single phase of deformed α'-martensite (Fig. 1b [12]).

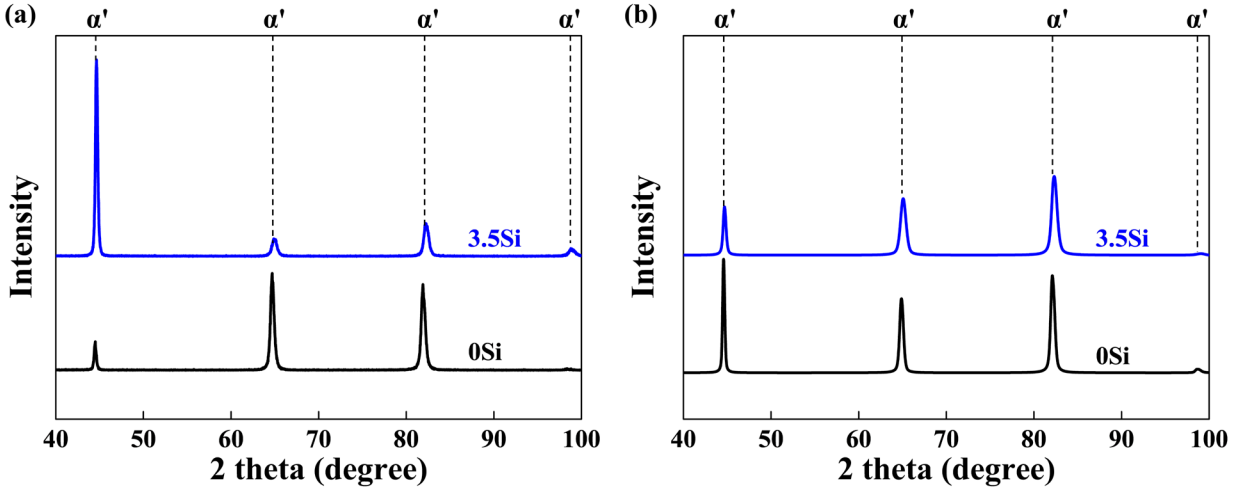

Fig. 1. *XRD patterns of (a) hot- and (b) cold-rolled present specimens [12].*

To evaluate the low-temperature superplasticity of the present steels, specimens were tensile-deformed at various temperatures with a $\dot{\varepsilon}$ of 1×10^{-3} s^{-1} (Fig. 2 [12]). The steels exhibited superplastic elongation above 300% at temperatures below 858 K (Fig. 2a [12]). Notably, the 3.5Si steel exhibited the lowest T_s of 763 K, which was confirmed by deforming the 0Si steel at 763 K

Materials Research Proceedings **32** (2023) 167-172 https://doi.org/10.21741/9781644902615-18

(Fig. 2b [12]). The 0Si steel showed lower engineering strain (76%) and higher peak stress than the 3.5Si steel, which indicates that the addition of 3.5wt% Si was effective in lowering the T_s.

Except for our steels, the lowest T_s of superplastic steels, above which the total elongation is 300% or over, is 873 K at a $\dot{\varepsilon}$ of 1×10^{-3} s^{-1} [1,2,7]. The 3.5Si steel exhibited the lowest T_s (763 K) [12], which is lower by 110 K than the lowest T_s (873 K) reported to date.

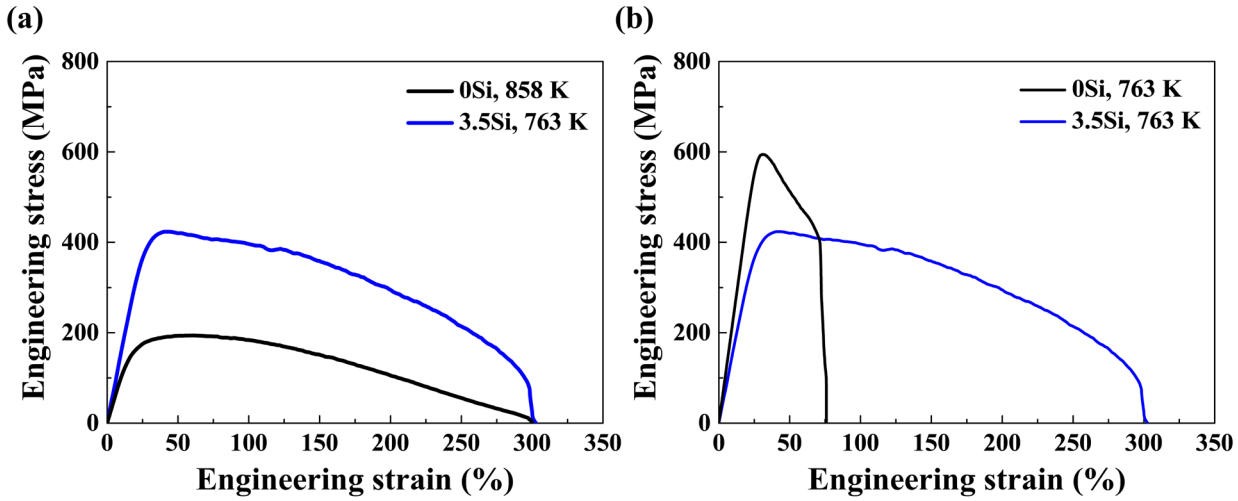

Fig. 2. *Engineering stress-strain curves of present steels measured (a) at the lowest temperature (T_s), where total elongation is 300% or over and (b) at 763 K [12].*

To elucidate the deformation mechanism responsible for the excellent superplasticity of 3.5Si steel, EBSD phase and grain orientation spread (GOS) maps were taken from the tensile-fractured 3.5Si specimen at 763 K (Fig. 3a). Ultrafine γ grains (~138 nm), which were absent before deformation, were observed on the phase map. This indicates that dynamic reverse transformation partially occurred during tensile deformation at 763 K. By comparing the phase map to the GOS map, fine recrystallized α grains with low GOS values [14] were distinguished. This confirms that the fine equiaxed grains shown in Fig. 3a consist of both recrystallized α and reverted γ grains.

However, the fraction of reverted γ grains was measured using XRD patterns due to the limited probing area of EBSD. For comparison, the fractions of recrystallized α and reverted γ grains were also measured using the 0Si specimen deformed at 763 K with a $\dot{\varepsilon}$ of 1×10^{-3} s^{-1}. As seen in Figs. 3b and c [12], the 3.5Si specimen exhibited remarkably higher fractions of recrystallized α grains and reverted γ grains than the 0Si specimen. In particular, the fraction of reverted γ grains increased linearly in 3.5Si steel during tensile deformation, reaching ~13% after failure.

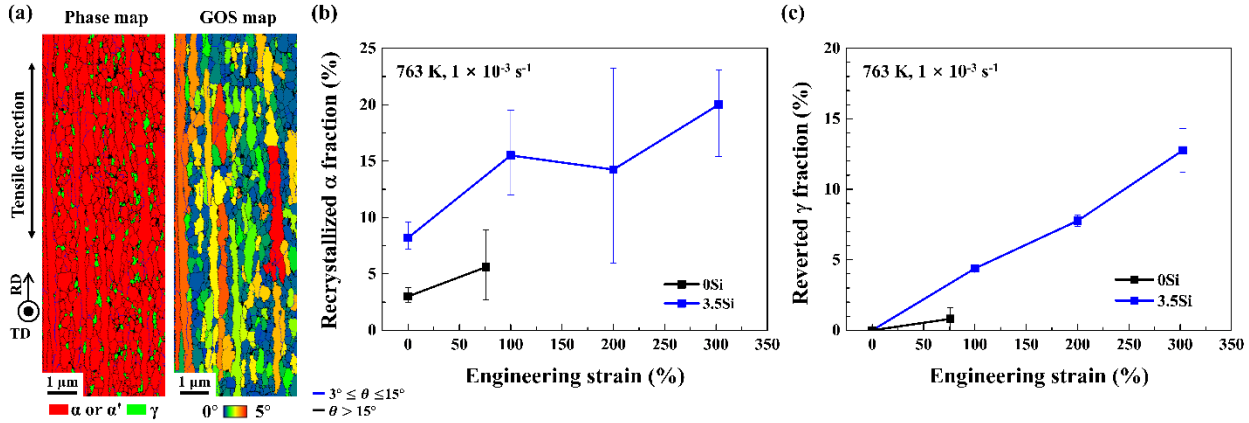

Fig. 3. *(a) EBSD maps of phase and GOS measured using the 303% deformed 3.5Si steel. Variations of the fractions of (b) recrystallized α grains [12] and (c) reverted γ grains with tensile strain in both 0Si and 3.5Si steel [12].*

According to Hashimoto *et al.*'s study [15], the sliding rate of the α/γ phase boundaries was significantly higher than that of α/α and γ/γ boundaries in a shear-deformed DSS bicrystal at 1373 K. Additionally, it is well-known that grain boundary sliding (GBS) actively occurs in superplastic materials with fine equiaxed grains [16]. Based on these, it can be inferred that GBS took place at the phase boundaries between the recrystallized α and reverted γ grains in the deformed 3.5Si steel, which had ultrafine recrystallized α (~307 nm) and reverted γ grains (~138 nm).

To reconfirm the occurrence of GBS, texture analysis was performed using the 3.5Si specimen strained by 303% at 763 K. While the orientation of recrystallized α grains revealed a texture component {114}<110> with an $I_{max.}$ of 5.9 (Fig. 4a), that of reverted γ grains exhibited a random texture with an $I_{max.}$ of 3.0 (Fig. 4b) due to GBS during tensile deformation at 763 K. It is considered that since not all recrystallized α grains were in contact with the reverted γ grains, they still exhibited slightly developed texture with $I_{max.}$ = 5.9 (Fig. 4a).

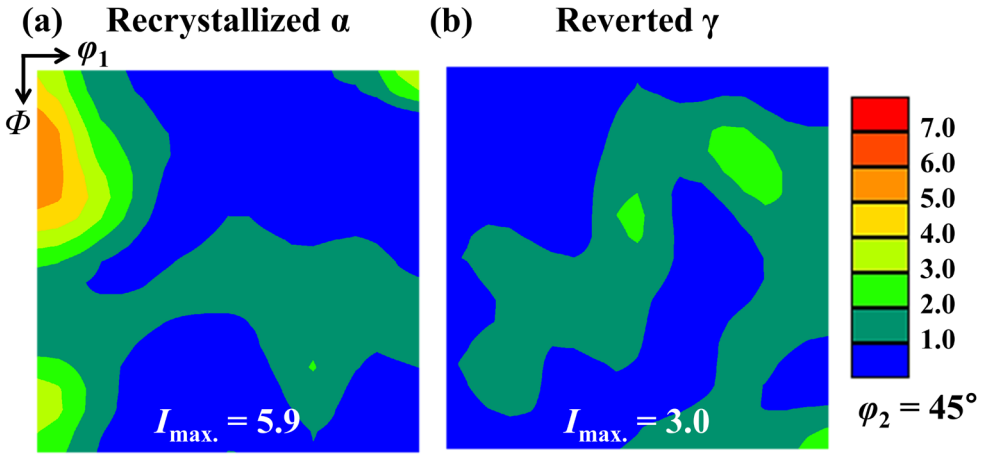

Fig. 4. *ODF maps of (a) recrystallized α and (b) reverted γ grains in the 3.5Si specimen deformed by 303% at 763 K with a $\dot{\varepsilon}$ of 1 × 10^{-3} s^{-1}.*

Meanwhile, the 3.5Si steel demonstrated an exceptional room-temperature tensile strength of 1336 MPa after undergoing superplastic forming simulation at 763 K (Fig. 5 [12]). Considering its numerous advantages, such as the lowest T_s, high room-temperature tensile strength, low material cost, and ease of fabrication, 3.5Si steel is considered an excellent option for producing mechanical parts that require complex shapes and high room-temperature tensile strength simultaneously.

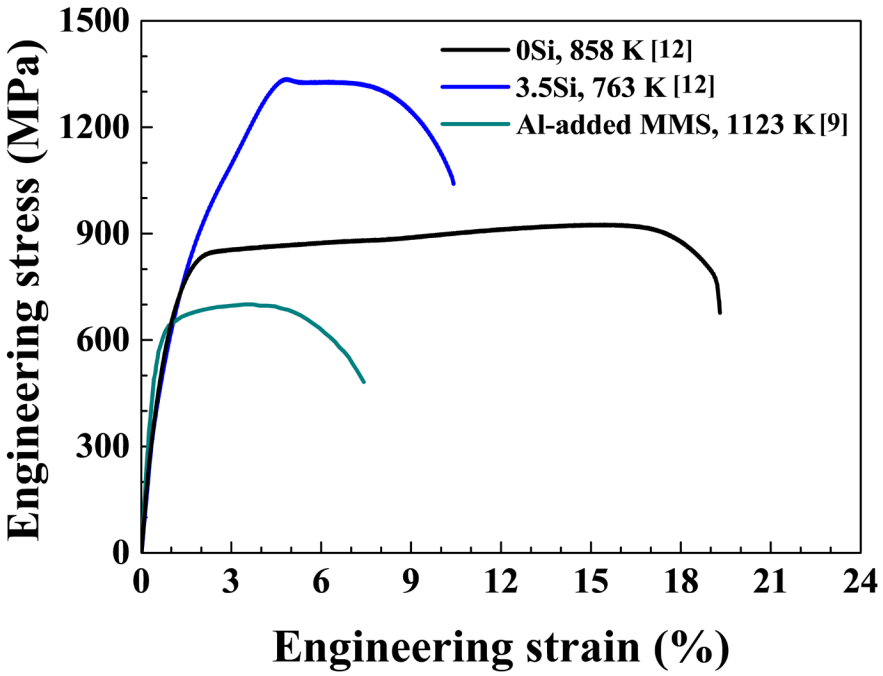

Fig. 5. *Engineering stress-strain curves measured at room temperature with a $\dot{\varepsilon}$ of 1 × 10^{-3} s^{-1} after the superplastic forming simulation [9,12].*

Summary

In the present study, we introduce a newly developed superplastic Fe-10Mn-3.5Si steel. The steel exhibited the lowest T_s of 763 K, which is 110 K lower than reported to date. The deformation mechanism of excellent superplasticity was GBS occurring at phase boundaries between recrystallized α and reverted γ grains. In addition, the steel showed remarkable room-temperature tensile strength. We suggest that this steel may accelerate the commercialization of superplastic steels.

References

[1] H. Zhang, D. Ponge, D. Raabe, Superplastic Mn-Si-Cr-C duplex and triplex steels: interaction of microstructure and void formation, Mater. Sci. Eng. A 610 (2014) 355-369. https://doi.org/10.1016/j.msea.2014.05.061

[2] H. Zhang, K.G. Pradeep, S. Mandal, D. Ponge, P. Choi, C.C. Tasan, D. Raabe, Enhanced superplasticity in an Al-alloyed multicomponent Mn-Si-Cr-C steel, Acta Mater. 63 (2014) 232-244. https://doi.org/10.1016/j.actamat.2013.10.034

[3] B. Walser, O.D. Sherby, Mechanical behavior of superplastic ultrahigh carbon steels at elevated temperature, Metall. Trans. A 10A (1979) 1461-1471. https://doi.org/10.1007/BF02812011

[4] Y.S. Han, S.H. Hong, The effects of thermos-mechanical treatments on superplasticity of Fe-24Cr-7Ni-3Mo-0.14N duplex stainless steel, Scr. Mater. 36 (1997) 557-563. https://doi.org/10.1016/S1359-6462(96)00421-6

[5] K. Tsuzaki, H. Matsuyama, M. Nagao, T. Maki, High-strain rate superplasticity and role of dynamic recrystallization in a superplastic duplex stainless steel, Mater. Trans., JIM 31 (1990) 983-994. https://doi.org/10.2320/matertrans1989.31.983

[6] W. Wang, M. Yang, D. Yan, P. Jiang, F. Yuan, X. Wu, Deformation mechanisms for superplastic behaviors in a dual-phase high specific strength steel with ultrafine grains, Mater. Sci. Eng. A 702 (2017) 133-141. https://doi.org/10.1016/j.msea.2017.07.011

[7] W. Cao, C. Huang, C. Wang, H. Dong, Y. Weng, Dynamic reverse phase transformation induced high-strain-rate superplasticity in low carbon low alloy steels with commercial potential, Sci. Rep. 7 (2017) 9199. https://doi.org/10.1038/s41598-017-09493-7

[8] Z. Cao, G. Wu, X. Sun, C. Wang, D. Ponge, W. Cao, Revealing the superplastic deformation behaviors of hot rolled 0.10C5Mn2Al steel with an initial martensitic microstructure, Scr. Mater. 152 (2018) 27-30. https://doi.org/10.1016/j.scriptamat.2018.03.046

[9] J. Han, S.-H. Kang, S.-J. Lee, M. Kawasaki, H.-J. Lee, D. Ponge, D. Raabe, Y.-K. Lee, Superplasticity in a lean Fe-Mn-Al steel, Nat. Commun. 8 (2017) 751. https://doi.org/10.1038/s41467-017-00814-y

[10] S.-H. Kang, S.-W. Choi, Y.-D. Im, Y.-K. Lee, Grain boundary sliding during high-temperature tensile deformation in superplastic Fe-6.6Mn-2.3Al steel, Mater. Sci. Eng. A 780 (2020) 139174. https://doi.org/10.1016/j.msea.2020.139174

[11] S.-H. Kang, H.-B. Jeong, J.-S. Hong, Y.-K. Lee, Effect of B on the superplasticity of Fe-6.6Mn-2.0Al alloy, Mater. Sci. Eng. A 822 (2021), 141697. https://doi.org/10.1016/j.msea.2021.141697

[12] H.-B. Jeong, S.-W. Choi, S.-H. Kang, Y.-K. Lee, Ultralow-temperature superplasticity of high strength Fe-10Mn-3.5Si steel, Mater. Sci. Eng. A 848 (2022) 143408. https://doi.org/10.1016/j.msea.2022.143408

[13] Y. Onuki, A. Hoshikawa, S. Sato, T. Ishigaki, T. Tomida, Quantitative phase fraction analysis of steel combined with texture analysis using time-of-flight neutron diffraction, J. Mater. Sci. 52 (2017) 11643-11658. https://doi.org/10.1007/s10853-017-1309-x

[14] V. Torganchuk, I. Vysotskiy, S. Malopheyev, S. Mironov, R. Kaibyshev, Microstructure evolution and strengthening mechanisms in friction-stir welded TWIP steel, Mater. Sci. Eng. A 746 (2019) 248-258. https://doi.org/10.1016/j.msea.2019.01.022

[15] S. Hashimoto, F. Moriwaki, T. Mimaki, S. Miura, Sliding along the interphase boundary in austenite/ferrite duplex stainless steel bicrystals, in: S. Hori (Ed.), Superplasticity in Advanced Materials, The Japan Soc. Res. on Superplasticity, 1991, pp. 23-32.

[16] K.A. Padmanabhan, S.B. Prabu, R.R. Mulyukov, A. Nazarov, R.M. Imayev, S. G. Chowdhury, Superplasticity: Common Basis for a Near-Ubiquitous Phenomenon, first ed., Springer, Berlin, Heidelberg, 2018. https://doi.org/10.1007/978-3-642-31957-0